Article

High aboveground carbon stock of African tropical montane forests

https://doi.org/10.1038/s41586-021-03728-4

Received: 20 December 2020

Accepted: 14 June 2021

Published online: 25 August 2021

Check for updates

A list of authors and affiliations appears at the end of the paper.

Tropical forests store 40–50 per cent of terrestrial vegetation carbon[1]. However, spatial variations in aboveground live tree biomass carbon (AGC) stocks remain poorly understood, in particular in tropical montane forests[2]. Owing to climatic and soil changes with increasing elevation[3], AGC stocks are lower in tropical montane forests compared with lowland forests[2]. Here we assemble and analyse a dataset of structurally intact old-growth forests (AfriMont) spanning 44 montane sites in 12 African countries. We find that montane sites in the AfriMont plot network have a mean AGC stock of 149.4 megagrams of carbon per hectare (95% confidence interval 137.1–164.2), which is comparable to lowland forests in the African Tropical Rainforest Observation Network[4] and about 70 per cent and 32 per cent higher than averages from plot networks in montane[2,5,6] and lowland[7] forests in the Neotropics, respectively. Notably, our results are two-thirds higher than the Intergovernmental Panel on Climate Change default values for these forests in Africa[8]. We find that the low stem density and high abundance of large trees of African lowland forests[4] is mirrored in the montane forests sampled. This carbon store is endangered: we estimate that 0.8 million hectares of old-growth African montane forest have been lost since 2000. We provide country-specific montane forest AGC stock estimates modelled from our plot network to help to guide forest conservation and reforestation interventions. Our findings highlight the need for conserving these biodiverse[9,10] and carbon-rich ecosystems.

Tropical forests cover less than 10% of the global land area yet store 40–50% of terrestrial vegetation carbon[1] and contribute more than one-third of primary productivity[11], so they are a key component of the global carbon cycle[12,13]. There is substantial variation in carbon stocks across the biome, with lowland forests in Africa and Borneo storing more carbon per unit area than lowland forests in the Neotropics[4,7]. This variation arises partly from structural differences: the signature feature of African forests is their low stem density but relatively high abundance of large trees (>70 cm in diameter), which store large quantities of carbon, whereas Bornean forests are characterized by high stem density and basal area[4,14,15].

Despite increased understanding of biogeographic differences in tropical lowland forests, patterns of spatial variation in carbon stocks remain poorly understood in the 880,000 km^2 of tropical montane forests located ≥1,000 m above sea level (a.s.l.)[2]. Montane forests are expected a priori to have lower aboveground live tree biomass carbon (AGC) stocks than lowland forests because (1) temperature decreases with increasing elevation, reducing net primary productivity and slowing nutrient recycling, (2) long periods of cloud immersion in montane forests suppresses productivity, (3) soil waterlogging slows nutrient recycling, and (4) high epiphyte load, local wind exposure in crests and nutrient-limited soils limit tree size and increase investment in roots over shoots[3]. Although forest inventory plots provide some support for these assumptions[2], data from African mountain regions are exceptionally sparse. Indeed, in the most recent Intergovernmental Panel on Climate Change (IPCC) guidelines, there is no specific AGC default value for old-growth montane forests in Africa: the value given of 89.3 MgC ha^{-1} is simply a mean of secondary and old-growth forests found at ≥1,000 m a.s.l. (ref. [8]). Mountain areas also pose special challenges for remote-sensing approaches for estimating carbon stocks, as radar data are affected by geometric distortions[16] and steep slopes bias spaceborne LiDAR estimates towards overestimating canopy height[17]. These issues are reflected in the limited correlation between estimates of AGC stocks at mountain locations from different recent remote-sensing-derived carbon maps (Supplementary Table 1).

Better understanding of montane carbon stocks is important for many African countries, particularly in eastern Africa where montane forests represent most of the extant evergreen old-growth forest cover. Quantifying carbon stocks in these ecosystems is critical for estimating national carbon losses from deforestation and forest degradation[18]. Quantifying carbon stocks in old-growth montane forests also serves to constrain potential carbon uptake by restored natural forests, given the high commitment of most African nations to the Bonn Challenge effort to restore 150 million hectares of degraded and deforested lands by 2020 (Table 1), and 350 million hectares by 2030.

Here we measured, compiled and analysed a new dataset of 226 plot inventories spanning 44 sites in 12 African countries, covering most major mountain regions on the continent (the 'AfriMont' dataset). Plots range from 800 m a.s.l. to 3,900 m a.s.l. to include submontane forests (800–1,000 m a.s.l.) in smaller mountains closer to the ocean[19,20]. For all plots, stem diameter and species were recorded for each tree ≥10 cm in diameter at breast height (or above buttress) following standard methods[21]. Tree height was sampled in 23 montane sites, allowing variation in height–diameter allometry to be incorporated into the calculation of aboveground biomass. A total of 72,336 stems with diameter ≥10 cm

Table 1 | Remaining forest area and AGC estimates for montane and lowland tropical forests in Africa

Country	Montane (ha)	Montane lost (ha)	Montane AGC ($Mg\ ha^{-1}$, 95% CI)	Montane sites (plots)	Lowland (ha)	Lowland AGC ($Mg\ ha^{-1}$, 95% CI)	Lowland plots	Bonn Challenge by 2020 (ha)
Burundi	25,000	300	94 (47–176)	1 (7)	0		0	2 million
Cameroon	840,000	30,200	153 (121–195)	7 (37)	17.7 million	166 (151–185)	72	12 million
Democratic Republic of the Congo	10.2 million	536,500	129 (84–202)	2 (37)	90 million	158 (135–183)	48	8 million
Ethiopia	1.7 million	62,100	165 (124–215)	8 (25)	145,000	[a]	0	15 million
Guinea	29,000	1,700	314 (147–616)[b]	1 (2)	193,000	157 (122– 206)[c]	24	2 million
Kenya	568,000	44,100	104 (79–136)	8 (38)	37,000		0	5.1 million
Mozambique	18,000	6,600[d]	226 (146–384)[b]	3 (4)	93,000	[e]	0	1 million
Nigeria	42,000	1,400	120 (47–309)[b]	1 (1)	1.8 million	161 (105–262)	2	4 million
Rwanda	53,000	300	106 (65–168)	2 (11)	0		0	2 million
Tanzania	587,000	13,900	175 (129–234)	6 (29)	130,000	128 (101–163)	16	5.2 million
Uganda	427,000	64,600[d]	158 (111–209)	6 (23)	18,000		0	2.5 million
Zimbabwe	7,000	800[d]	203 (108–363)	1 (12)	<1,000		0	2 million

Forest cover circa 2018 was extracted from ref. [38] and clipped to 'primary humid forest' using ref. [39]. Montane forest lost covers the period 2000–2018. Mean aboveground carbon (AGC, in $MgC\ ha^{-1}$) estimates for montane (or lowland) forests were estimated from AfriMont and AfriTRON plot network data. AGC values are means with 95% confidence intervals in parentheses. For details on sites and plots used, see Supplementary Table 5. Bonn Challenge pledges for 2030 are not yet available.

[a]Ref. [48] reports 192 $MgC\ ha^{-1}$ for lowland.

[b]Few plots sampled, or very small plots sampled, AGC estimates may not be robust; see Extended Data Fig. 10.

[c]Data from neighbouring Liberia.

[d]Montane forest loss in Mozambique, Uganda and Zimbabwe represents 27%, 13% and 10% of the existing montane forest in 2001, respectively. Montane forest loss in Côte d'Ivoire (no plot data are available) was estimated to be 21% for the same period.

[e]Ref. [49] reports 132.2 $MgC\ ha^{-1}$ for lowland.

were measured. For each tree, we computed AGC (in $MgC\ ha^{-1}$) according to standard procedures (Methods).

We find that the mean plot-level AGC stock across the sampled African tropical montane forests is 149.4 $MgC\ ha^{-1}$ (95% confidence interval (CI) 137.1–164.2), two-thirds more than the IPCC default value of 89.3 $MgC\ ha^{-1}$. Our estimates are robust to subsampling our dataset (Extended Data Fig. 1) and excluding small plots (Extended Data Fig. 2), and are not affected by the sampling strategy used to establish plots in each study site (Extended Data Fig. 2). Comparing our dataset to previous syntheses of montane[2,5,6] and lowland[7] forest plot networks reveals that tropical montane forests in Africa have significantly higher AGC stocks per unit area than both montane (95% CI 50.4–71.9 $MgC\ ha^{-1}$) and lowland (95% CI 124.0–147.9 $MgC\ ha^{-1}$) forests in the Neotropics, and that they do not differ significantly from lowland forests in Africa (95% CI −27.6–9.6 $MgC\ ha^{-1}$) (Fig. 1, Supplementary Table 2). The similar AGC stocks in montane and lowland forests in Africa contrasts with the Neotropics and Southeast Asia, where carbon stocks are lower in montane forests than lowland forests (albeit not significantly different in Southeast Asia due to the small sample size) (Fig. 1). These differences are robust to accounting for differences in elevation among montane datasets: removing African plots 800–1,000 m a.s.l. slightly reduces estimated montane forest AGC stock to 145.0 $MgC\ ha^{-1}$ (95% CI 129.6–163.2), but observed differences in AGC stock among continents remain when plots are restricted to elevations that are well represented in all continents (Extended Data Fig. 3).

The characteristic structural properties of lowland African forests (relatively low stem density and greater importance of large trees compared with elsewhere in the tropics[4]) are also evident in the African montane forests we sampled. In these montane forests, the mean stem density is 483.3 stems per hectare (±177.7 s.d.) and the mean basal area is 39 $m^2\ ha^{-1}$ (±14.8 s.d.). We find a high density of large stems (>70 cm in diameter, 19.1 stems per hectare ± 15.4 s.d.), which contribute 35.3% (95% CI 29.6–41.8%) to plot-level AGC stock (Fig. 2). The contribution of large trees to plot-level AGC stock is also similar in montane and lowland Africa (95% CI of difference in square-root transformed proportional contribution of large trees between lowland and montane forests −0.100–0.075, $P = 0.80$). There was no significant difference in the proportional contribution of any other size class to AGC stocks between our montane dataset and 132 lowland plots from the African Tropical Rainforest Observatory Network (AfriTRON; $P \geq 0.24$) (Supplementary Table 3), although greater variation among plots is observed in montane forests (Fig. 2).

To investigate whether elevation affected AGC or forest structure, we modelled these variables as functions of elevation using random slopes mixed-effects models. This approach allows intercepts and relationships to vary among sites, which would be expected as mountains can have very different climate at the same elevation owing to proximity to the ocean (generally the farther, the drier) and because of the mass-elevation or telescopic effect[22] (larger mountains are better at warming the atmosphere above them). We found that AGC, stem density or density of large stems (>70 cm in diameter) were not significantly related to elevation (Fig. 3, Supplementary Table 4). Across sites, these non-significant relationships were all negative, although there was some variation in strength and direction among sites (Fig. 3). Similarly, in the Neotropics and Southeast Asia montane forest plot datasets, AGC was not significantly correlated with elevation (Extended Data Fig. 4).

To assess potential environmental drivers of AGC-stock variation across the AfriMont plot network, we related AGC to climate, soil and topography. We found that AGC stocks increased with annual precipitation (albeit not statistically significantly), decreased with soil fertility and were higher in plots that were locally at higher elevation than their surroundings (Extended Data Fig. 5). Relationships with other environmental variables were non-significant (Extended Data Fig. 5). Although global datasets might not capture fine-scale variation in climate or soils in mountain regions[23], leading to regression dilution[24], the general absence of strong climate effects combined with the lack of a significant effect of elevation on AGC stocks suggest that the high AGC stock of African montane forests is a pervasive phenomenon across a wide environmental gradient.

Although the AfriMont dataset covers most major mountain areas in tropical Africa (Fig. 4), some areas remain under-sampled relative

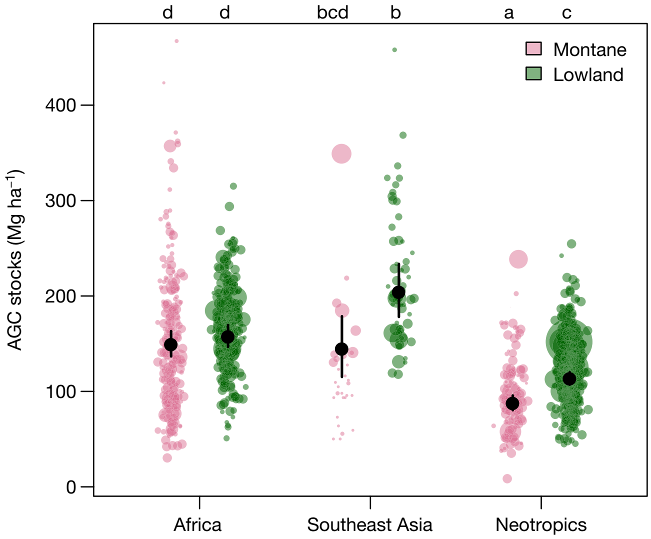

Fig. 1 | Pantropical variation in AGC stocks sampled by plot networks in montane (≥800 m a.s.l.) and lowland (<800 m a.s.l.) tropical forests. Data for African montane forests (n = 226 plots, this study), montane forests in the Neotropics (n = 131) and Southeast Asia (n = 32) are from refs. [2,5,6] and data for lowland forests in Africa (n = 290), the Neotropics (n = 416) and Southeast Asia (n = 60) are from ref. [7]. The coloured points show the AGC stock in each plot, with point size proportional to square-root plot area. The black points show means for each continent–elevation category estimated using linear mixed-effects models with site as a random effect, and lines show 95% confidence intervals around means. The lowercase letters indicate significant differences between continent–elevation category combinations (linear mixed-effects models with site as a random effect, P < 0.05).

to forest extents (Extended Data Fig. 6), resulting in some differences between the environmental conditions sampled by our plot network and the wider montane forest biome in Africa (Extended Data Fig. 7). Notably, the absence of plots from montane forests of eastern Democratic Republic of the Congo (Fig. 4, Extended Data Fig. 6) means that the AfriMont dataset samples forests are, on average, at higher elevations, and are cooler and cloudier than the wider montane forest biome in Africa (Extended Data Fig. 7). Using relationships with environmental variables (Extended Data Fig. 5) to predict AGC stocks in each 1-km grid cell containing montane forest gives a mean (weighted by remaining forest cover) AGC stock of 176.9 MgC ha^{-1} (±32.0 s.d.) for the tropical montane forest biome in Africa. This indicates that the estimate we report based on our AfriMont plot network data (149.4 MgC ha^{-1}) is conservative.

Several mechanisms could explain the high AGC stock of montane forests in the AfriMont plot network. First, large herbivores such as elephants (*Loxodonta* spp.) can have marked effects on forest structure by consuming biomass, destroying small stems, dispersing seeds and transporting nutrients[25]. Studies for lowland forests suggest that elephants can increase carbon stocks[26,27]. We tested whether AfriMont plots with a known elephant presence as of 2019 had significantly higher AGC stocks, but found that they had significantly lower AGC stocks, although significant differences were not observed in some countries (Extended Data Fig. 8). Although the initial ecosystem response to elephant removal might be greater AGC stocks due to reduced biomass consumption and small-stem destruction, the longer-term effects might differ. We were unable to fully disentangle such effects, as we lacked details on both the time since elephant extirpation and the elephant abundance and its determinants (Supplementary Table 5).

A second potential explanation is a relatively low frequency of large-scale abiotic disturbances, allowing trees time to grow large and stands to self-thin, as is seen in lowland African forests[4]. For example, tropical cyclones are largely absent in mainland Africa (except in Mozambique[28]) and lava flows are limited even in the active volcano of Mount Cameroon[29]. Although fine-scale variability in landslide risk limits comparisons across large spatial scales, there are fewer areas with high landslide susceptibility in mountains in tropical Africa than in the Andes and most mountain ranges in Southeast Asia[30]. If forests have been ecologically stable over evolutionary timescales, tree species may be adapted to grow slowly but potentially reaching great sizes[31]. On Mount Kilimanjaro *Entandrophragma* individuals reach enormous heights and ages[32]. This low frequency of large-scale abiotic disturbances contrasts with the Andes and several mountains in Southeast Asia (for example, Barisian mountains in western Sumatra), which are tectonically active, so the trees there are adapted to sudden disturbance followed by intense competition to get established and grow. Future monitoring of the AfriMont plot network will help to determine the extent to which the high biomass of African tropical montane forests results from them being dynamic and productive, or adapted to stability.

A third potential explanation could be the presence of conifers[33]. Mixed conifer/broadleaved forests tend to have a greater basal area than purely broadleaved forests owing to a more effective use of light and other resources[34]. Podocarpaceae can be found in montane forests across the tropics[35]. Despite having fewer species in Africa than in other continents[36], these could be more abundant at the site level. However, there is no pantropical comparative study on Podocarpaceae abundance in tropical montane forests. In our dataset, there was no significant correlation between plot-level AGC stock and conifer (Podocarpaceae) abundance (Extended Data Fig. 9). Other explanations could be continental differences in mountain terrain (more gentle slopes or plateau regions in Africa) or types of montane forest investigated (less cloud forest existing/sampled in Africa). Within our dataset, slope did not have a significant effect on AGC stocks (Extended Data Fig. 5). Contrary to the Neotropics[37], there is no high-resolution map of cloud forests available for Africa, so although we found no relationship between AGC stock and cloud frequency (Extended Data Fig. 5), we were unable to investigate differences in AGC stock between cloud forest and non-cloud forest plots.

To understand the policy implications of our findings for African countries, we calculated montane (≥800 m a.s.l.) forest cover change between 2000 and 2018, using forest cover from ref. [38] and clipped to 'primary humid forest' from ref. [39]. We show that tropical montane forests represent most—or all—evergreen old-growth forests found in ten African countries (Fig. 4), and that the Democratic Republic of the Congo has two-thirds of the remaining 16 million hectares of montane forests in Africa. Over 0.8 million hectares (5%) have been lost in Africa since 2001, with the highest losses in the Democratic Republic of the Congo (536,000 ha), Uganda (65,000 ha) and Ethiopia (62,000 ha) (Fig. 4, Table 1). In terms of percentage, Mozambique and Côte d'Ivoire lost over 20% of their montane forests over this period (Fig. 4, Table 1). In some sites, however, a larger proportion of montane forests was lost before 2000, for example, in Taita Hills in Kenya[40]. If absolute country-level deforestation rates continue, a further 0.5 million hectares of tropical montane forests will be lost by 2030.

African tropical montane forests are not only carbon rich but also contain some of the highest concentrations of biodiversity and endemism in the world[9,10]. They are important 'water towers' as—located at the headwaters of numerous river systems, including the Congo and the Nile—they regulate the timing and magnitude of runoff[9]. They also regulate local temperatures[41] and provide numerous other services to people in the surrounding landscapes[9]. Clearly, more should be done to avoid the destruction of these important ecosystems. Logging, mining and clearing land for farming, but also political unrest and militia presence, have affected—and continue

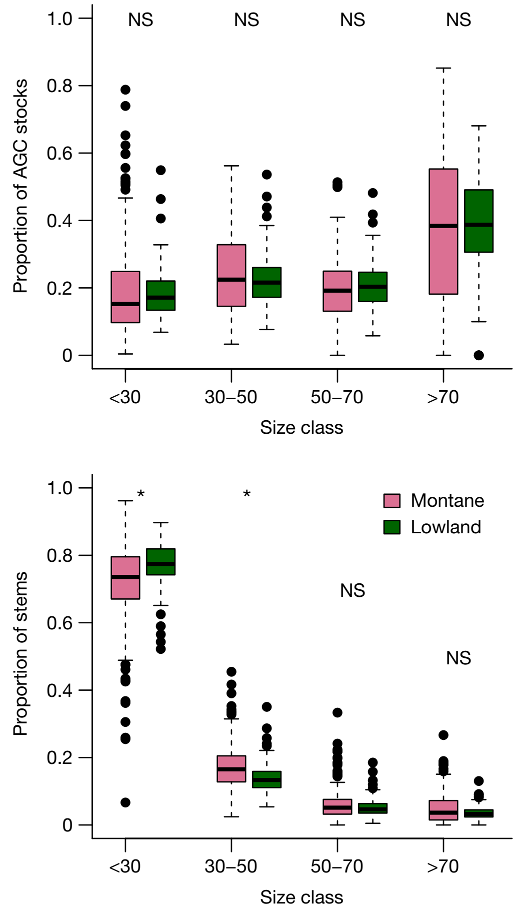

Fig. 2 | Proportion of plot-level AGC stock and stems accounted for by each size class in montane and lowland forests in Africa. Statistically significant differences in the contribution of each size class between montane and lowland forest plot networks are shown by asterisks (linear mixed-effects model, $P < 0.05$). NS, non-significant difference. Montane, $n = 226$; lowland, $n = 132$. The thick line shows the median, and boxes cover the interquartile range (IQR). Values >1.5 times IQR away from the IQR are shown by points.

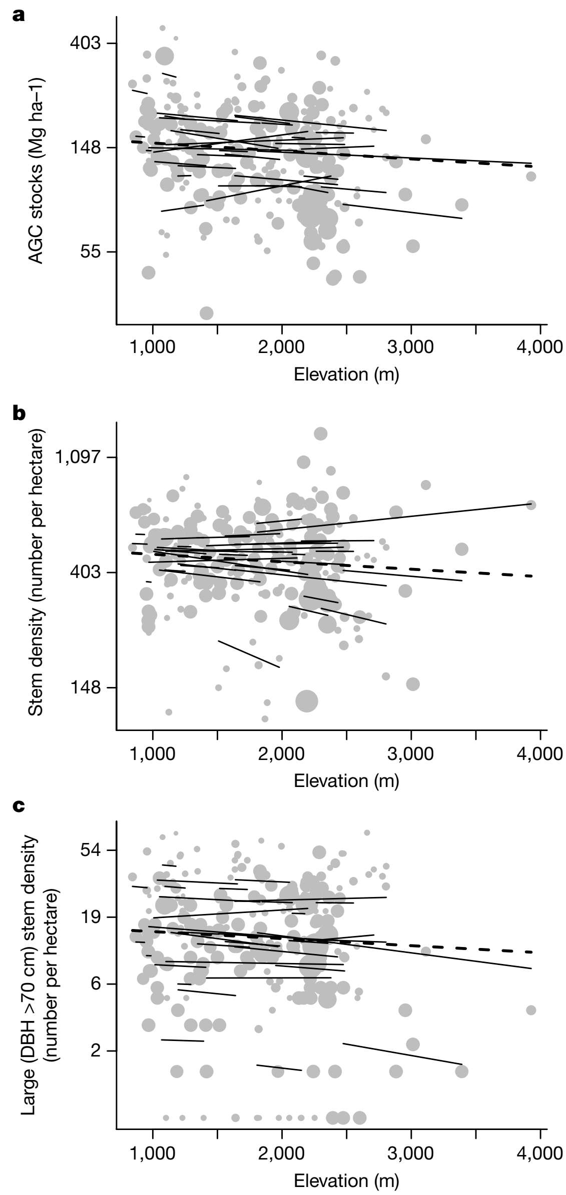

Fig. 3 | Variables as a function of elevation. a–c, Relationship between elevation and plot-level AGC stock (**a**), stem density (**b**) and stem density of large stems (>70 cm diameter) (**c**) for the AfriMont dataset. Note the log scale of *y* axis. Each response variable was log-transformed and modelled as a function of elevation with a linear mixed-effect models with random slopes. The dashed line shows the relationship across sites (non-significant in all cases, $P \geq 0.3$) (Supplementary Table 4) and the solid lines show the relationship within each site. The point sizes are proportional to square-root plot area. A polynomial model allowing a nonlinear relationship with elevation was also tested but not supported over the linear model in any case ($P \geq 0.7$) (Supplementary Table 4). The absence of a significant relationship with elevation is robust to removing the two highest elevation sites, Rwenzori and Virunga (Supplementary Table 4). DBH, diameter at breast height.

to affect—these forests, for example, in Itombwe Mountains in the Democratic Republic of the Congo[42]. Protected areas are known to help to reduce deforestation in the tropics[43]. Beyond protected areas, other forest conservation mechanisms could be implemented, including effective carbon finance. Previous IPCC AGC-stock estimates for montane forests in Africa (89.3 MgC ha^{-1}) may have contributed to low incentives for carbon finance mechanisms in these ecosystems. Our study shows the far greater carbon-storage potential in these tropical montane forests, which will be even higher if soil carbon stocks are considered (for example, >200 MgC ha^{-1} of organic carbon occurs in the top 0–30 cm of soil on Mount Cameroon[44] and in the Usambara Mountains, Tanzania[45]).

As well as conserving the remaining montane forests, efforts to restore them are critical. Forest restoration at one of our sites, Kibale National Park in Uganda, indicates the potential for rapid AGC accumulation[46]. Our study shows the high potential AGC stock these montane forests can attain. The possible co-benefits of forest restoration, notably water regulation, control of soil erosion and landslides, and biodiversity conservation should also be considered. Most African nations are committed to the Bonn Challenge; Ethiopia leading with 15 million hectares committed (Table 1). We provide country-specific estimates of potential AGC stocks based on forests sampled in the AfriMont dataset to help guide such interventions (Table 1, Extended Data Fig. 10). Caution is needed when scaling-up our estimates to the landscape scale, as not all forests are closed-canopy old-growth and structurally intact. Remote-sensing or ancillary data (landcover maps and spatial environmental data) could be used to identify, for example, exotic plantations, degraded or bamboo forests, and thus help to create detailed AGC maps at different spatial scales[18,47]. A closer collaboration between airborne, spaceborne and ground approaches (such as the AfriMont and AfriTRON plot networks) is key for accurate quantification and monitoring of landscape-scale tropical forest AGC stocks, particularly in mountain regions.

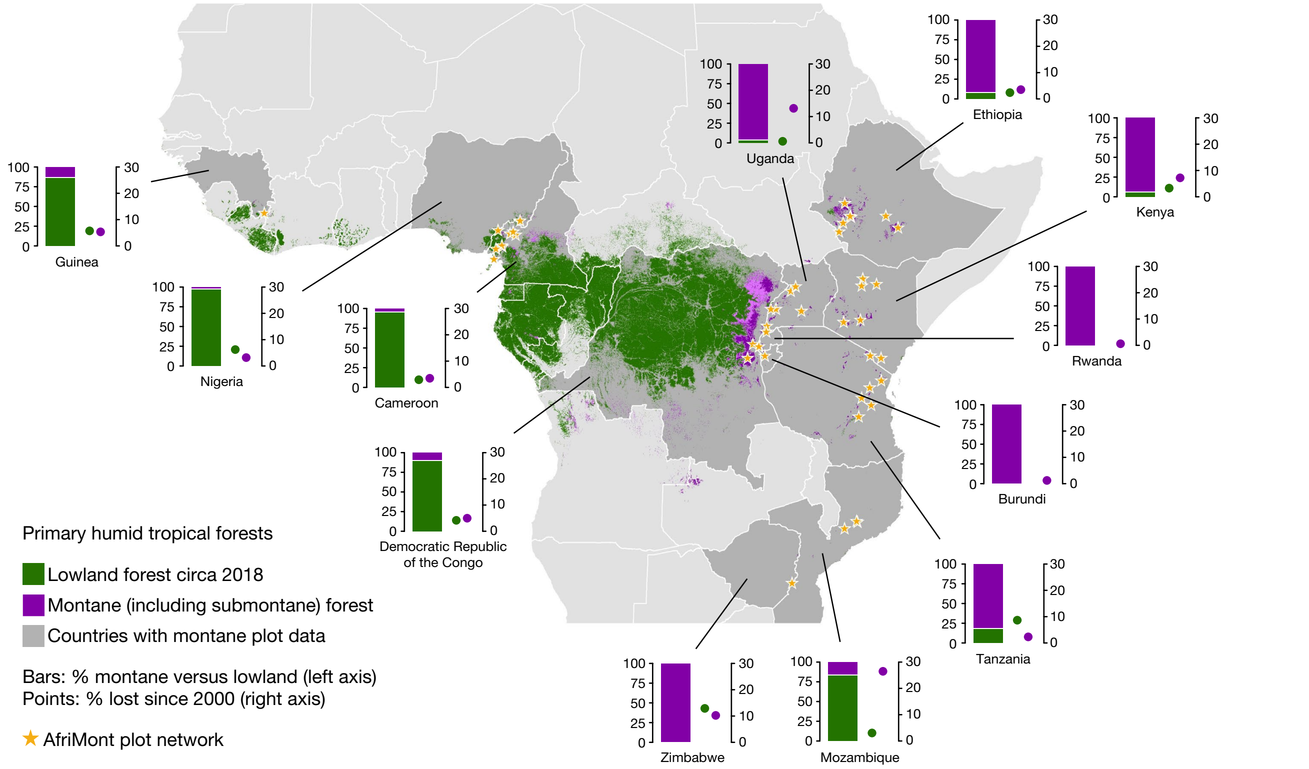

Fig. 4 | Old-growth evergreen humid forests in lowland and montane tropical Africa. Forest extent circa 2018. Montane includes submontane forests (800–1,000 m a.s.l., light purple). Montane forests represent most (or all) evergreen humid old-growth forest in ten African nations: Burundi, Ethiopia, Kenya, Rwanda, Tanzania, Uganda and Zimbabwe (included in AfriMont); and Zambia, Malawi and South Sudan (no plot data available). Forest cover extracted from ref. [38] and clipped to 'primary humid forest' using ref. [39]. See Table 1 for country-level absolute estimates.

Our newly compiled dataset and analysis provides a large-scale quantification of AGC stock in African tropical montane forests, indicating it to be on average substantially higher than previously thought. Although there is variation around this mean AGC stock within and across sites, it is not systematically related to elevation. Apart from helping refine country-level estimates, IPCC guidelines and ground calibration of remote-sensing estimates, continued on-the-ground monitoring of the AfriMont plot network will help determine ecosystem dynamics and carbon residence time in these extraordinarily carbon-rich forests, as well as their responses to climatic changes.

Online content

Any methods, additional references, Nature Research reporting summaries, source data, extended data, supplementary information, acknowledgements, peer review information; details of author contributions and competing interests; and statements of data and code availability are available at https://doi.org/10.1038/s41586-021-03728-4.

1. Erb, K. et al. Unexpectedly large impact of forest management and grazing on global vegetation biomass. *Nature* **553**, 73–76 (2018).
2. Spracklen, D. V. & Righelato, R. Tropical montane forests are a larger than expected global carbon store. *Biogeosciences* **11**, 2741–2754 (2014).
3. Fahey, T. J., Sherman, R. E. & Tanne, E. V. J. Tropical montane cloud forest: environmental drivers of vegetation structure and ecosystem function. *J. Trop. Ecol.* **32**, 355–367 (2016).
4. Lewis, S. L. et al. Above-ground biomass and structure of 260 African tropical forests. *Phil. Trans. R. Soc. Lond. B* **368**, 20120295 (2013).
5. Vilanova, E. et al. Environmental drivers of forest structure and stem turnover across Venezuelan tropical forests. *PLoS ONE* **13**, e0198489 (2018).
6. Álvarez-Dávila, E. et al. Forest biomass density across large climate gradients in northern South America is related to water availability but not with temperature. *PLoS ONE* **12**, e0171072 (2017).
7. Sullivan, M. J. P. et al. Long-term thermal sensitivity of Earth's tropical forests. *Science* **368**, 869–874 (2020).
8. Domke, G. et al. in 2019 *Refinement to the 2006 IPCC Guidelines for National Greenhouse Gas Inventories* Vol. 4 (eds Calvo Buendia, E. et al.) Ch. 4, 48 (IPCC, 2019).
9. *African Mountains Atlas* (UNEP, 2014).
10. Rahbek, C. et al. Humboldt's enigma: what causes global patterns of mountain biodiversity? *Science* **365**, 1108–1113 (2019).
11. Pan, Y. et al. A large and persistent carbon sink in the world's forests. *Science* **333**, 988–993 (2011).
12. Booth, B. B. B. et al. High sensitivity of future global warming to land carbon cycle processes. *Environ. Res. Lett.* **7**, 024002 (2012).
13. Hubau, W. et al. Asynchronous carbon sink saturation in African and Amazonian tropical forests. *Nature* **579**, 80–87 (2020).
14. Feldpausch, T. R. et al. Tree height integrated into pantropical forest biomass estimates. *Biogeosciences* **9**, 3381–3403 (2012).
15. Bastin, J.-F. et al. Pan-tropical prediction of forest structure from the largest trees. *Glob. Ecol. Biogeogr*. **27**, 1366–1383 (2018).
16. *CCI BIOMASS Product User Guide Year 1 Version 1.0,* https://climate.esa.int/sites/default/files/biomass_D4.3_Product_User_Guide_V1.0.pdf (Aberystwyth University and GAMMA Remote Sensing, 2019).
17. Lefsky, M. A., Keller, M., Pang, Y., de Camargo, P. & Hunter, M. O. Revised method for forest canopy height estimation from the Geoscience Laser Altimeter System waveforms. *J. Appl. Remote Sens.* **1**, 013537 (2007).
18. Willcock, S. et al. Quantifying and understanding carbon storage and sequestration within the Eastern Arc Mountains of Tanzania, a tropical biodiversity hotspot. *Carbon Balance Manag*. **9**, 2 (2014); correction **12**, 20 (2017).
19. Bussmann, R. W. Vegetation zonation and nomenclature of African Mountains—an overview. *Lyonia* **11**, 41–66 (2006).
20. Hamilton, A. Vegetation, climate and soil, altitudinal relationships on the East Usambara Mountains of Tanzania. *J. East Afr. Nat. Hist*. **87**, 85–89 (1998).
21. Phillips, O., Baker, T., Brienen, R. & Feldpausch, T. *RAINFOR Field Manual for Plot Establishment and Remeasurement,* http://www.rainfor.org/upload/ManualsEnglish/RAINFOR_field_manual_version_2016.pdf (Univ. Leeds, 2016)
22. Jarvis, A. & Mulligan, M. The climate of cloud forests. *Hydrol. Process.* **25**, 327–343 (2011).
23. Platts, P. J., Omeny, P. A. & Marchant, R. AFRICLIM: high-resolution climate projections for ecological applications in Africa. *Afr. J. Ecol*. **53**, 103–108 (2015).
24. McInerny, G. J. & Purves, D. W. Fine-scale environmental variation in species distribution modelling: regression dilution, latent variables and neighbourly advice. *Methods Ecol. Evol.* **2**, 248–257 (2011).
25. Poulsen, J. R. et al. Ecological consequences of forest elephant declines for Afrotropical forests. *Conserv. Biol.* **32**, 559–567 (2018).
26. Berzaghi, F. et al. Carbon stocks in central African forests enhanced by elephant disturbance. *Nat. Geosci.* **12**, 725–729 (2019); correction **12**, 1050 (2019).
27. Enquist, B. J. et al. The megabiota are disproportionately important for biosphere functioning. *Nat. Commun.* **11**, 699 (2020).

28. Lin, T.-C., Hogan, J. A. & Chang, C. T. Tropical cyclone ecology: a scale-link perspective. *Trends Ecol. Evol*. **35**, 594–604 (2020).
29. Favalli, M. et al. Lava flow hazard and risk at Mt. Cameroon volcano. *Bull. Volcanol*. **74**, 423–439 (2012).
30. Stanley, T. & Kirschbaum, D. B. A heuristic approach to global landslide susceptibility mapping. *Nat. Hazards* **87**, 145–164 (2017).
31. Lovett, J. C. Elevational and latitudinal changes in tree associations and diversity in the Eastern Arc mountains of Tanzania. *J. Trop. Ecol*. **12**, 629–650 (1996).
32. Hemp, A. et al. Africa's highest mountain harbours Africa's tallest trees. *Biodivers. Conserv*. **26**, 103–113 (2017).
33. Culmsee, H., Leuschner, C., Moser, G. & Pitopang, R. Forest aboveground biomass along an elevational transect in Sulawesi, Indonesia, and the role of Fagaceae in tropical montane rain forests. *J. Biogeogr*. **37**, 960–974 (2010).
34. Enright, N. J. & Ogden, J. in *Ecology of the Southern Conifers* (eds Enright, N. J. & Hill, R. S.) 271–287 (Melbourne Univ. Press, 1995).
35. Neale, D. B. & Wheeler, N. C. in *The Conifers: Genomes, Variation and Evolution* (eds Neale, D. B. & Wheeler, N. C.) 1–21 (Springer, 2019).
36. Mill, R. R. Towards a biogeography of the Podocarpaceae. *Acta Hortic*. **615**, 137–147 (2003).
37. Helmer, E. H. et al. Neotropical cloud forests and paramo to contract and dry from declines in cloud immersion and frost. *PLoS ONE* **14**, e0213155 (2019).
38. Hansen, M. C. et al. High-resolution global maps of 21st-century forest cover change. *Science* **342**, 850–853 (2013).
39. Turubanova, S., Potapov, P., Tyukavina, A. & Hansen, M. Ongoing primary forest loss in Brazil, Democratic Republic of the Congo, and Indonesia. *Environ. Res. Lett*. **13**, 074028 (2018).
40. Pellikka, P. K. E., Lötjönen, M., Siljander, M. & Lens, L. Airborne remote sensing of spatiotemporal change (1955–2004) in indigenous and exotic forest cover in the Taita Hills, Kenya. *Int. J. Appl. Earth Obs. Geoinf*. **11**, 221–232 (2009).
41. Zeng, Z. et al. Deforestation-induced warming over tropical mountain regions regulated by elevation. *Nat. Geosci*. **14**, 23–29 (2021).
42. Spira, C., Kirkby, A., Kujirakwinja, D. & Plumptre, A. J. The socio-economics of artisanal mining and bushmeat hunting around protected areas: Kahuzi–Biega National Park and Itombwe nature reserve, eastern Democratic Republic of Congo. *Oryx* **53**, 136–144 (2019).
43. Bebber, D. P. & Butt, N. Tropical protected areas reduced deforestation carbon emissions by one third from 2000–2012. *Sci. Rep*. **7**, 14005 (2017); **8**, 14845 (2018).
44. Tegha, K. C. & Sendze, Y. G. Soil organic carbon stocks in Mt Cameroon National Park under different land uses. *J. Ecol. Nat. Environ*. **8**, 20–30 (2016).
45. Munishi, P. K. T. & Shear, T. H. Carbon storage in afromontane rain forests of the eastern arc mountains of Tanzania: their net contribution to atmospheric carbon. *J. Trop. For. Sci*. **16**, 78–98 (2004).
46. Wheeler, C. E. et al. Carbon sequestration and biodiversity following 18 years of active tropical forest restoration. *For. Ecol. Manage*. **373**, 44–55 (2016).
47. Avitabile, V., Baccini, A., Friedl, M. A. & Schmullius, C. Capabilities and limitations of Landsat and land cover data for aboveground woody biomass estimation of Uganda. *Remote Sens. Environ*. **117**, 366–380 (2012).
48. Aneseyee, B. A., Soromessa, T. & Belliethathan, S. Carbon sock of Gambella National Park: implication for climate change mitigation. *Int. J. Adv. Life Sci*. **35**, 41–56 (2015).
49. Lisboa, S. N. et al. Biomass allometric equation and expansion factor for a mountain moist evergreen forest in Mozambique. *Carbon Balance Manag*. **13**, 23 (2018).

Publisher's note Springer Nature remains neutral with regard to jurisdictional claims in published maps and institutional affiliations.

Aida Cuni-Sanchez[1,2]✉, Martin J. P. Sullivan[3,4], Philip J. Platts[1,5,6], Simon L. Lewis[4,7], Rob Marchant[1], Gérard Imani[8], Wannes Hubau[9,10], Iveren Abiem[11,12], Hari Adhikari[13], Tomas Albrecht[14,15], Jan Altman[16], Christian Amani[8], Abreham B. Aneseyee[17,18], Valerio Avitabile[19], Lindsay Banin[20], Rodrigue Batumike[21], Marijn Bauters[22], Hans Beeckman[9], Serge K. Begne[4,23], Amy C. Bennett[4], Robert Bitariho[24], Pascal Boeckx[22], Jan Bogaert[25], Achim Bräuning[26], Franklin Bulonvu[27], Neil D. Burgess[28], Kim Calders[29], Colin Chapman[30,31,32,33], Hazel Chapman[12,34], James Comiskey[35], Thales de Haulleville[36], Mathieu Decuyper[37,38], Ben DeVries[39], Jiri Dolezal[16,40], Vincent Droissart[23,41], Corneille Ewango[42], Senbeta Feyera[43], Aster Gebrekirstos[44], Roy Gereau[45], Martin Gilpin[4], Dismas Hakizimana[46], Jefferson Hall[47], Alan Hamilton[48], Olivier Hardy[49], Terese Hart[50], Janne Heiskanen[13,51], Andreas Hemp[52], Martin Herold[38,53], Ulrike Hiltner[26,54], David Horak[55], Marie-Noel Kamdem[23], Charles Kayijamahe[56], David Kenfack[47], Mwangi J. Kinyanjui[57], Julia Klein[58], Janvier Lisingo[42], Jon Lovett[4], Mark Lung[59], Jean-Remy Makana[60], Yadvinder Malhi[61], Andrew Marshall[1,62,63], Emanuel H. Martin[64], Edward T. A. Mitchard[65], Alexandra Morel[66], John T. Mukendi[9], Tom Muller[67], Felix Nchu[68], Brigitte Nyirambangutse[69,70], Joseph Okello[22,71,72], Kelvin S.-H. Peh[73,74], Petri Pellikka[13,75], Oliver L. Phillips[4], Andrew Plumptre[76], Lan Qie[77], Francesco Rovero[78,79], Moses N. Sainge[80], Christine B. Schmitt[81,82], Ondrej Sedlacek[55], Alain S. K. Ngute[62,83], Douglas Sheil[84], Demisse Sheleme[85], Tibebu Y. Simegn[86], Murielle Simo-Droissart[23], Bonaventure Sonké[23], Teshome Soromessa[17], Terry Sunderland[87,88], Miroslav Svoboda[89], Hermann Taedoumg[90,91], James Taplin[92], David Taylor[93], Sean C. Thomas[94], Jonathan Timberlake[95], Darlington Tuagben[96], Peter Umunay[97], Eustrate Uzabaho[56], Hans Verbeeck[29], Jason Vleminckx[98], Göran Wallin[70], Charlotte Wheeler[65], Simon Willcock[99,100], John T. Woods[101] & Etienne Zibera[69]

[1]Department of Environment and Geography, University of York, York, UK. [2]Department of International Environmental and Development Studies (NORAGRIC), Norwegian University of Life Sciences, Ås, Norway. [3]Department of Natural Sciences, Manchester Metropolitan University, Manchester, UK. [4]School of Geography, University of Leeds, Leeds, UK. [5]Leverhulme Centre for Anthropocene Biodiversity, University of York, York, UK. [6]Climate Change Specialist Group, Species Survival Commission, International Union for Conservation of Nature, Gland, Switzerland. [7]Department of Geography, University College London, London, UK. [8]Biology Department, Université Officielle de Bukavu, Bukavu, Democratic Republic of the Congo. [9]Service of Wood Biology, Royal Museum for Central Africa, Tervuren, Belgium. [10]Department of Environment, Laboratory of Wood Technology (Woodlab), Ghent University, Ghent, Belgium. [11]University of Jos, Jos, Nigeria. [12]Nigerian Montane Forest Project, Yelwa Village, Nigeria. [13]Department of Geosciences and Geography, University of Helsinki, Helsinki, Finland. [14]Department of Zoology, Faculty of Science, Charles University, Prague, Czech Republic. [15]Institute of Vertebrate Biology, Czech Academy of Sciences, Brno, Czech Republic. [16]Institute of Botany of the Czech Academy of Science, Třeboň, Czech Republic. [17]College of Natural and Computational Science, Addis Ababa University, Addis Ababa, Ethiopia. [18]Department of Natural Resource Management, College of Agriculture and Natural Resource, Wolkite University, Wolkite, Ethiopia. [19]European Commission, Joint Research Centre, Ispra, Italy. [20]UK Centre for Ecology and Hydrology, Edinburgh, UK. [21]Université du Cinquantenaire Lwiro, Département de sciences de l'environnement, Kabare, Democratic Republic of the Congo. [22]Isotope Bioscience Laboratory (ISOFYS), Ghent University, Ghent, Belgium. [23]Plant Systematic and Ecology Laboratory, Higher Teachers' Training College, University of Yaoundé I, Yaoundé, Cameroon. [24]Institute of Tropical Forest Conservation, Mbarara University of Science and Technology, Mbarara, Uganda. [25]Biodiversity and Landscape Unit, Gembloux Agro-Bio Tech, Université de Liege, Liège, Belgium. [26]Institute for Geography, Friedrich Alexander University, Erlangen–Nuremberg, Germany. [27]Département de Eaux et Forêts, Institut Supérieur d'Agroforesterie et de Gestion de l'Environnement de Kahuzi-Biega (ISAGE-KB), Kalehe, Democratic Republic of the Congo. [28]UN Environment World Conservation Monitoring Center (UNEP-WCMC), Cambridge, UK. [29]Computational and Applied Vegetation Ecology (CAVElab), Faculty of Bioscience Engineering, Ghent University, Ghent, Belgium. [30]Department of Anthropology, George Washington University, Washington DC, USA. [31]School of Life Sciences, University of KwaZulu-Natal, Pietermaritzburg, South Africa. [32]Shaanxi Key Laboratory for Animal Conservation, Northwest University, Xi'an, China. [33]International Centre of Biodiversity and Primate Conservation, Dali University, Dali, China. [34]University of Canterbury, Canterbury, New Zealand. [35]Inventory and Monitoring Program, National Park Service, Fredericksburg, VA, USA. [36]University of Ghent, Ghent, Belgium. [37]World Agroforestry (ICRAF), Nairobi, Kenya. [38]Laboratory of Geo-Information Science and Remote Sensing, Wageningen University, Wageningen, The Netherlands. [39]Geography, Environment and Geomatics, University of Guelph, Guelph, Ontario, Canada. [40]Faculty of Science, University of South Bohemia, České Budějovice, Czech Republic. [41]AMAP Lab, Université de Montpellier, IRD, CNRS, INRAE, CIRAD, Montpellier, France. [42]Faculté de Gestion de Ressources Naturelles Renouvelables, Université de Kisangani, Kisangani, Democratic Republic of the Congo. [43]College of Development Studies, Addis Ababa University, Addis Ababa, Ethiopia. [44]Dendrochronology Laboratory, World Agroforestry Centre (ICRAF), Nairobi, Kenya. [45]Missouri Botanical Garden, St Louis, MO, USA. [46]Department of Biology, University of Burundi, Bujumbura, Burundi. [47]Smithsonian Institution Forest Global Earth Observatory (ForestGEO), Smithsonian Tropical Research Institute, Washington DC, USA. [48]Kunming Institute of Botany, Kunming, China. [49]Université Libre de Bruxelles, Brussels, Belgium. [50]Division of Vertebrate Zoology, Yale Peabody Museum of Natural History, New Haven, CT, USA. [51]Institute for Atmospheric and Earth System Research, Faculty of Science, University of Helsinki, Helsinki, Finland. [52]Department of Plant Systematics, University of Bayreuth, Bayreuth, Germany. [53]Helmholtz Center Potsdam GFZ German Research Centre for Geosciences, Section 1.4 Remote Sensing and Geoinformatics, Potsdam, Germany. [54]Helmholtz-Centre for Environmental Research (UFZ), Leipzig, Germany. [55]Department of Ecology, Faculty of Science, Charles University, Prague, Czech Republic. [56]International Gorilla Conservation Programme, Musanze, Rwanda. [57]Department of Natural Resources, Karatina University, Karatina, Kenya. [58]Department of Ecosystem Science and Sustainability, Colorado State University, Fort Collins, CO, USA. [59]Eco2librium LLC, Boise, ID, USA. [60]Department of Ecology, Université de Kisangani, Kisangani, Democratic Republic of the Congo. [61]Environmental Change Institute, School of Geography and the Environment, University of Oxford, Oxford, UK. [62]Tropical Forests and People Research Centre, University of the Sunshine Coast, Sippy Downs, Queensland, Australia. [63]Flamingo Land Ltd, Malton, UK. [64]College of African Wildlife Management, Mweka, Tanzania. [65]School of GeoSciences, University of Edinburgh, Edinburgh, UK. [66]Department of Geography and Environmental Sciences, University of Dundee, Dundee, UK. [67]Independent Botanist, Harare, Zimbabwe. [68]Department of Horticultural Sciences, Faculty of Applied Sciences, Cape Peninsula University of Technology, Bellville, South Africa. [69]Biology Department, University of Rwanda, Kigali, Rwanda. [70]Department of Biological and Environmental Sciences, University of Gothenburg, Gothenburg, Sweden. [71]Mountains of the Moon University, Fort Portal, Uganda. [72]National Agricultural Research Organisation, Mbarara Zonal Agricultural Research and Development Institute, Mbarara, Uganda. [73]School of Biological Sciences, University of Southampton, Southampton, UK. [74]Conservation Science Group, Department of Zoology, University of Cambridge, Cambridge, UK. [75]State Key Laboratory of Information Engineering in Surveying, Mapping and Remote Sensing, Wuhan University, Wuhan, China. [76]Key Biodiversity Areas Secretariat, BirdLife International, Cambridge, UK. [77]School of Life Sciences, University of Lincoln, Lincoln, UK. [78]Department of Biology, University of Florence, Sesto Fiorentino, Italy. [79]Tropical Biodiversity Section, Museo delle Scienze, Trento, Italy.

[80]Tropical Plant Exploration Group (TroPEG), Mundemba, Cameroon. [81]Center for Development Research (ZEF), University of Bonn, Bonn, Germany. [82]Conservation and Landscape Ecology, University of Freiburg, Freiburg, Germany. [83]Applied Biology and Ecology Research Unit, University of Dschang, Dschang, Cameroon. [84]Forest Ecology and Forest Management Group, Wageningen University, Wageningen, The Netherlands. [85]Water and Land Resources Center, Addis Ababa University, Addis Ababa, Ethiopia. [86]African Wildlife Foundation (AWF), Biodiversity Conservation and Landscape Management Program, Simien Mountains National Park, Debark, Ethiopia. [87]Faculty of Forestry, University of British Columbia, Vancouver, British Columbia, Canada. [88]Center for International Forestry Research (CIFOR), Bogor, Indonesia. [89]Department of Forest Ecology, Faculty of Forestry and Wood Sciences, Czech University of Life Sciences, Prague, Czech Republic. [90]Department of Plant Biology, Faculty of Sciences, University of Yaoundé I, Yaoundé, Cameroon. [91]Bioversity International, Yaoundé, Cameroon. [92]UK Research and Innovation, London, UK. [93]Department of Geography, National University of Singapore, Singapore, Singapore. [94]Institute of Forestry and Conservation, University of Toronto, Toronto, Ontario, Canada. [95]Biodiversity Foundation for Africa, East Dean, UK. [96]Forestry Development Authority of the Government of Liberia (FDA), Monrovia, Liberia. [97]School of Forestry and Environmental Studies, Yale University, New Haven, CT, USA. [98]Department of Biological Sciences, Florida International University, Miami, FL, USA. [99]School of Natural Sciences, University of Bangor, Bangor, UK. [100]Rothamsted Research, Harpenden, UK. [101]University of Liberia, Monrovia, Liberia.
✉e-mail: a.cuni-sanchez@york.ac.uk

Methods

AfriMont or montane Africa dataset

We compiled forest inventory plot data from AfriTRON (www.afritron.org), with data curated at www.ForestPlots.net[50,51] and the TEAM network[52], as well as from numerous site-specific publications detailed in Supplementary Table 5 and mapped in Fig. 4. Plots were selected for the analysis when conforming to the following criteria: ≥800 m a.s.l., closed-canopy evergreen wet or moist tropical forest, geo-referenced, old-growth and structurally intact (not affected by recent selective logging, fire or coffee cultivation), with no exotic species present (for example, *Eucalyptus* or *Pinus* spp.), all trees ≥10 cm in diameter measured and majority of stems identified to species. We included plots from Virunga Massif in Rwanda/Uganda even when not 100% closed canopy due to the high abundance of naturally occurring bamboo. In all plots, tree diameter was measured at 1.3 m along the stem from the ground, or above buttresses if present. In 23 sites, tree height was sampled in the field for some stems, using a clinometer or a laser. Families and species names follow the African Plant Database (http://africanplantdatabase.ch). The AfriMont dataset consists of 72,336 stems, of which 92.9% were identified to species, 98.4% to genus and 98.5% to family. This dataset represents a standardized safe long-term repository of valuable historical data (four sites initially considered could not be included because tree-level data had already been lost by data owners).

AfriTRON or lowland Africa dataset

The 132 lowland forest plots are all from AfriTRON[4,13,53]. They were selected using the same criteria as above (but with elevation <800 m a.s.l.), restricted to countries for which we also had montane plots plus neighbouring countries where the mountains span international borders (for example, Mount Nimba spans Guinea and Liberia). The dataset includes 51,305 stems, of which 89.6% were identified to species, 97.3% to genus and 97.7% to family. The plot data were retrieved from www.ForestPlots.net on 6 January 2019. The plot locations and details are in Supplementary Table 6.

Literature dataset

We compiled data on AGC stocks in tropical lowland and montane forests to compare with the AfriMont data. Data for lowland forests came from ref. [7]. and consisted of all multi- and single-census plots that were <800 m a.s.l. Data for montane forests were obtained from ref. [2], with additional data from Venezuela[5] and Colombia[6]. Montane plots were defined as ≥800 m a.s.l.; elevation was not provided for the Colombian dataset so plots were selected based on the forest type, and these plots were excluded from analyses requiring elevation. To avoid double counting plots, Venezuelan and Colombian plots were removed from the ref. [2] dataset.

Aboveground carbon

For each tree in the montane dataset, we used the published allometric equation by ref. [54] to estimate aboveground biomass. This allometric equation was created using data from directly harvested trees at 58 sites across the tropics, including eight sites with elevation ≥800 m a.s.l. (range 900–3,000 m a.s.l. including sites in Africa). We then converted this biomass to carbon, assuming that AGC (in MgC ha^{-1}) is 45.6% of aboveground biomass[55]. AGC for each plot was estimated as the sum of the AGC of each living stem, divided by planimetric plot area (in hectares). If field measurements of slope were unavailable, we converted surface to planimetric area extracting slope from the NASA's Shuttle Radar Topography Mission (SRTM) product. We excluded tree ferns, bamboo and palms, as these were not measured in all plots. Reference[54] includes tree diameter, wood mass density and tree height. The best taxonomic match wood density of each stem was extracted from a global database[56,57] following ref. [53]. For some sites, all trees in a plot had been sampled for height. If this was not the case, but some field measurements of height were available (typically ten stems per diameter class), we constructed a site-specific height–diameter model, using a Weibull equation following ref. [14]. If no field measurements of height were available, we constructed a cluster-specific height–diameter model, using a Weibull equation, as explained in Supplementary Table 7. The same approach was used to calculate aboveground biomass for lowland forests. For these, height was estimated using a Weibull equation following ref. [14].

Small plots and data subsampling

For 22 sites where plots were small (<0.2 ha), we aggregated plots to groups of about 0.2 ha based on their geographic proximity, elevation, environmental affinity and the co-authors' knowledge of the site, to help reduce the variation among plots at site level. This is because the presence of an extremely large tree in a small plot can result in overestimates of AGC[58]. We investigated whether using the aggregated-plot approach affected AGC-stock estimates at the site level, and this was not the case (Extended Data Fig. 2). We also investigated whether including small plots affected the continental mean AGC-stock estimates, as small plots have greater edge surface, and there is a tendency of some field teams to include large trees inside plots when laying out the boundaries[59]. Including small plots did not significantly affect our continental mean AGC-stock estimates (Extended Data Fig. 2). We also explored the sensitivity of our continental mean AGC-stock estimates to data subsampling. Data were resampled at different sample sizes either at plot level (sampling with replacement) or at site level (sampling without replacement). The number of plots ($n = 226$) and the number of sites ($n = 44$) we sampled indicate that our estimates of AGC stock at the continental level are robust (Extended Data Fig. 1). They are also not affected by the fact that we included plots 800–1,000 m a.s.l. (Extended Data Fig. 3).

Size classes

For all plots, we computed the proportion of AGC that was distributed in each size-diameter class, using the classes of ref. [15]. We also computed stem density, basal area, density of large trees (>70 cm in diameter, named SD_{70} in stems per hectare) and Podocarpaceae abundance (in percentage of plot-level basal area).

Environmental variables and their effects

Climate variables (temperature annual mean and seasonality, and precipitation mean and seasonality, that is, Bio1, Bio4, Bio12 and Bio15) were extracted from WorldClimV2[60] at 30-arcsec (about 1 km) resolution. Mean temperature values were adjusted for the difference in elevation between the plot and the wider 1-km grid cell using the lapse rate of −0.005 °C m^{-1}. We obtained data on cloud cover from ref. [61] and lightning frequency (0.1°, about 11 km) from the Lightning Imaging Sensor (LIS) very-high-resolution climatology[62]. Values for soil variables (cation exchange capacity, CEC, representing soil fertility, and percentage clay representing soil texture) were extracted from SoilGrids[63] (about 1-km resolution) and a depth-weighted mean taken for values from 0 cm to 30 cm depth to give a single value of each soil variable per plot. Elevation was obtained from SRTM (at 3-arcsec resolution, about 90 m). Topographic metrics were calculated from elevation data using the terrain function in the raster R package version 3.3-6. These were slope and topographic position index (TPI). The TPI is the difference between the elevation of the plot and the mean value of the eight surrounding grid cells—positive values indicate locally high locations and negative values indicate locally low locations. Where small plots were aggregated for analysis, environmental variables were extracted for the ungrouped plot locations, and then an area-weighted mean taken to obtain a plot-level value.

Elephant and conifer effects on AGC stocks

For the current elephant presence in the AfriMont plots, we created a binary variable (presence/absence) based on co-authors' knowledge of elephant ranges and elevation distribution at each site as of 2019. Co-authors estimated that elephants were present in 2019 in 54 plots in 12 sites in five countries (Supplementary Table 5). For all plots that had at least one individual in the Podocarpaceae family (47 plots, 16 sites, 7 countries), we computed the contribution of Podocarpaceae to plot basal area and AGC stock in terms of percentages.

Estimating forest cover and loss

We obtained estimates of forest cover and loss in the years 2000 to 2018, using the 'loss year' dataset of the Global Forest Change database, version 1.6 (ref. [38]). To exclude plantation forests, 'dry' forests (for example, miombo woodland) and degraded forests, we applied the 'primary humid forest' mask developed by ref. [39]. We distinguished montane from lowland forests using an elevational cut-off of 800-m elevation, using the SRTM v3 product at 1-arcsec resolution (snapping to the ref. [38] grid of the same resolution). Where there were gaps in the 1-arcsec SRTM product, we filled these using a 1-arcsec bilinear interpolation of the (gapless) 3-arcsec SRTM product. Areal estimates of forest cover and loss were calculated at 30-m resolution using the Africa sinusoidal projection. To estimate future forest loss by 2030, we extrapolated absolute country-level deforestation rates for the period 2000–2018 (in hectares per year).

Investigating AfriMont representativeness

To quantify AfriMont sampling effort within the montane forest biome in Africa, we used the map of tropical montane forest extent (see above) and calculated the amount of remaining forest in each 1° grid cell. By dividing the area sampled in the AfriMont dataset by the proportion of this biome in a grid cell, we calculated the expected sampling intensity if sampling was proportional to remaining forest extent. To assess how representative our plot network was of the environmental conditions of the wider tropical montane forest biome in Africa, we extracted the environmental data (climate and soil variables presented above) at about 1-km resolution from grid cells that contained montane forest. We then visually compared the distribution of each variable in our dataset to its distribution across the biome (Extended Data Fig. 7).

AfriMont versus global AGC maps

We extracted alternative AGC estimates for the AfriMont plots (unaggregated, $n = 666$) from four different sources: Harris et al.[64] (30-m resolution, dated 2000), the European Space Agency Climate Change Initiative Biomass map[65] (100-m resolution, 2017), Saatchi, et al.[66] (1-km resolution, 2007–2008) and Avitabile et al.[67] (1-km resolution, circa 2000–2010). Most of the AfriMont plots were sampled between 2000 and 2019 (Supplementary Table 5). Where the plots were found within a single map pixel, we extracted that value. Where plots were larger than the pixel size, we averaged the values from the surrounding pixels weighted according to the proportion of the pixel that was in the plot.

Statistical analysis

Data were analysed using linear mixed-effects models, with site as a random effect. Site was included as a random intercept in all models, and as a random slope where relationships were assessed against elevation. Allowing the slope of the elevation effect to vary among sites in this way captures the a priori expectation for slopes to differ among sites, for example, due to mass-elevation effects. The effect of plot size on variation was accounted for by weighting observations by a power transformation of plot size; this was estimated during model fitting using the varPower function in the nlme R package[68], and then models refitted using the lme4 R package[69] using these estimated weights. Confidence intervals and P values for mixed-effects model parameters were estimated by bootstrapping models (1,000 iterations) using the bootstrap_parameters function in the parameters R package[70]. AGC stocks, stem density and SD_{70} were natural-log transformed (a small constant was added to SD_{70} before log-transforming to avoid log-transforming zeros) to meet assumptions of normality and avoid heteroscedacity. Likewise, the proportional contribution of each size class was square-root transformed. Differences in AGC stocks between all combinations of lowland and montane forests among continents were assessed using Tukey post hoc tests implemented in the multcomp R package[71]. Relationships between AGC stocks and environmental variables were investigated by fitting all subsets of the full model with all environmental covariates and averaging the best supported (difference in Akaike information criterion from the best supported model <4) models (using dredge and movel.avg functions in the MuMIn R package[72]. We used these relationships with climate and soil to predict AGC stocks in each 1-km grid cell containing montane forests (holding topographic variables at their dataset wide mean), and then took the forest-area weighted mean of these to obtain a single mean for the tropical montane forest biome in Africa. Differences in AGC stocks between plots with and without elephants were tested using a t-test with AGC stocks natural-log transformed. We investigated whether Podocarpaceae abundance (in terms of basal area) and plot AGC stocks were significantly correlated using Spearman's rank correlation coefficient. To investigate whether the sampling design affected AfriMont AGC-stock estimates, we used analysis of variance to test whether site-level mean AGC stocks differed according to the sampling strategy used to establish plots at that site. To explore the relationship between AfriMont AGC-stock estimates and global maps, and among these global maps, we used Spearman's rank correlation test.

Data availability

Source data to generate figures and tables are available from https://doi.org/10.5521/forestplots.net/2021_5.

Code availability

The R code to generate figures and tables is available from https://doi.org/10.5521/forestplots.net/2021_5.

50. Lopez-Gonzalez, G., Lewis, S. L., Burkitt, M. & Phillips, O. L. ForestPlots.net: a web application and research tool to manage and analyse tropical forest plot data. *J. Veg. Sci.* **22**, 610–613 (2011).
51. Lopez-Gonzalez, G., Lewis, S. L., Burkitt, M., Baker, T. R. & Phillips, O. L. *ForestPlots.net Database,* http://www.forestplots.net (ForestPlots, 2009).
52. Cavanaugh, K. et al. Carbon storage in tropical forests correlates with taxonomic diversity and functional dominance on a global scale. *Glob. Ecol. Biogeogr*. **23**, 563–573 (2014).
53. Lewis, S. L. et al. 2009 Increasing carbon storage in intact African tropical forests. *Nature* **457**, 1003–1006 (2009).
54. Chave, J. et al. Improved allometric models to estimate the aboveground biomass of tropical trees. *Glob. Change Biol*. **20**, 3177–3190 (2014).
55. Martin, A. R., Doraisami, M. & Thomas, S. C. Global patterns in wood carbon concentration across the world's trees and forests. *Nat. Geosci*. **11**, 915–920 (2018).
56. Chave, J. et al. Towards a worldwide wood economics spectrum. *Ecol. Lett*. **12**, 351–366 (2009).
57. Zanne, A. E. et al. Towards a worldwide wood economics spectrum. *Dryad* https://doi.org/10.5061/dryad.234 (2009).
58. Clark, D. A. et al. Net primary production in tropical forests: an evaluation and synthesis of existing field data. *Ecol. Appl*. **11**, 371–384 (2001).
59. Paul, T. S. H., Kimberley, M. O. & Beets, P. N. Thinking outside the square: evidence that plot shape and layout in forest inventories can bias estimates of stand metrics. *Methods Ecol. Evol*. **10**, 381–388 (2019).
60. Fick, S. E. & Hijmans, R. J. WorldClim 2: new 1-km spatial resolution climate surfaces for global land areas. *Int. J. Climatol*. **37**, 4302–4315 (2017).
61. Wilson, A. M. & Jetz, W. Remotely sensed high-resolution global cloud dynamics for predicting ecosystem and biodiversity distributions. *PLoS Biol*. **14**, e1002415 (2016).
62. Albrecht, R., Goodman, S., Buechler, D., Blakeslee R. & Christian, H. *LIS 0.1 Degree Very High Resolution Gridded Lightning Climatology Data Collection,* https://ghrc.nsstc.nasa.gov/pub/lis/climatology/LIS/ (NASA Global Hydrology Resource Center, 2016).
63. Hengl, T. et al. SoilGrids250m: global gridded soil information based on machine learning. *PLoS ONE* **12**, e0169748 (2017).
64. Harris, N. L. et al. Global maps of twenty-first century forest carbon fluxes. *Nat. Clim. Chang*. **11**, 234–240 (2021).
65. Santoro, M. & Cartus, O. *ESA Biomass Climate Change Initiative (Biomass_cci): Global Datasets of Forest Above-ground Biomass for the year 2017, v1* (Centre for Environmental Data Analysis, 2019).
66. Saatchi, S. et al. Benchmark map of forest carbon stocks in tropical regions across three continents. *Proc. Natl Acad. Sci. USA* **108**, 9899–9904 (2011).

67. Avitabile, V. et al. An integrated pan-tropical biomass map using multiple reference datasets. *Glob. Change Biol.* **22**, 1406–1420 (2016).
68. Pinheiro, J., Bates, D., DebRoy, S., Sarkar, D. & R Core Team nlme: linear and nonlinear mixed effects models. R package version 3.1-151 (2020).
69. Bates, D., Maechler, M., Bolker B. & Walker, S. Fitting linear mixed-effects models using lme4. *J. Stat. Softw.* **67**, 1–48 (2015).
70. Lüdecke, D., Ben-Shachar, M., Patil, I. & Makowski, D. Parameters: extracting, computing and exploring the parameters of statistical models using R. *J. Open Source Softw.* **5**, 2445 (2020).
71. Hothorn, T., Bretz, F. & Westfall, P. Simultaneous inference in general parametric models. *Biom. J.* **50**, 346–363 (2008).
72. Barton, K. MuMIn: multi-model inference. R package version 1.43.17 (2020)

Acknowledgements We thank the people of the many villages and local communities who welcomed our field teams and became our field assistants, without whose support the AfriMont dataset would not have been possible. Cameroon: villages Elak-Oku, Bokwoango, Bakingili, Muandelengoh, Enyandong, Ekangmbeng, Ngalmoa, Dikome Balue, Muyange, Matamani; assistants E. Ndive, D. Wultof, F. Keming, E. Bafon, J. Meyeih, T. K. Konsum, J. Esembe, F. Luma, F. Teke, E. E. Dagobert, E. D. Ndode, N. F. Njikang; Democratic Republic of the Congo: Bunyakiri, J. Kalume, W. Gului, D. Cirhagaga, B. Mugisho. Kenya: assistants A. M. Aide, H. Lerapo, J. Harugura, R. A. Wamuro, J. Lekatap, L. Lemooli, D. Kimuzi, B. M. Lombo, J. Broas, J. Hietanen, V. Heikinheimo, E. Schäfer. Rwanda: assistants I. Rusizana, P. Niyontegereje, J. B. Gakima, F. Ngayabahiga. Tanzania: TEAM staff and affiliates. Uganda: K. Laughlin, X. Mugumya, L. Etwodu, M. Mugisa. For logistical and administrative support, we are indebted to international, national and local institutions: SOPISDEW, Mt Cameroon National Park, Tropical Plant Exploration Group (TroPEG), Institut Congolais de Conservation de la Nature, Kahuzi-Biega National Park, Itombwe Nature Reserve, NEMA Marsabit Office, Taita Research Station, Kenya Forest Service, Rwanda Development Board, Nyungwe National Park, Conservation International, the Smithsonian Institution, Wildlife Conservation Society, Sokoine University of Agriculture, Tanzania Wildlife Research Institute, Tanzania National Parks Authority, Kilimanjaro National Park, Tanzania Commission for Science and Technology, Royal Zoological Society of Scotland, Uganda Wildlife Authority, Makerere University Biological Field Station, Uganda National Forestry Authority and Uganda National Council for Science and Technology. Field campaigns for AfriMont were funded by Marie Skłodowska-Curie Actions Intra-European Fellowships (number 328075) and Global Fellowships (number 74356), National Geographic Explorer (NGS-53344R-18), Czech Science Foundation (number 21-17125S), Rufford Small Grant Foundation (16712-B, 19476-D), Ministry of Foreign Affairs of Finland (BIODEV project), the Academy of Finland (number 318645), Swedish International Development Cooperation Agency, the Leverhulme Trust, the Strategic Research Area Biodiversity and Ecosystem Services in a Changing Climate, the German Research Foundation (DFG), Gatsby Plants, Natural Science and Engineering Research Council of Canada and International Development Research Centre of Canada. This paper is also a product of the AfriTRON network, for which we are indebted to hundreds of institutions, field assistants and local communities for establishing and maintaining the plots, including the Forestry Development Authority of the Government of Liberia, the University of Liberia, University of Ibadan (Nigeria), the University of Abeokuta (Nigeria), the University of Yaounde I (Cameroon), the National Herbarium of Yaounde (Cameroon), the University of Buea (Cameroon), Bioversity International (Cameroon), Salonga National Park (Democratic Republic of Congo), The Centre de Formation et de Recherche en Conservation Forestière (CEFRECOF, Epulu, Democratic Republic of Congo), the Institut National pour l'Étude et la Recherche Agronomiques (INERA, Democratic Republic of Congo), the École Régionale Postuniversitaire d'Aménagement et de Gestion intégrés des Forêts et Territoires tropicaux (ERAIFT Kinshasa, Democratic Republic of Congo), WWF-Democratic Republic of Congo, WCS-Democratic Republic of Congo, the Université de Kisangani (Democratic Republic of Congo), Université Officielle de Bukavu (Democratic Republic of Congo), Université de Mbujimayi (Democratic Republic of Congo), le Ministère de l'Environnement et Développement Durable (Democratic Republic of Congo), the FORETS project in Yangambi (CIFOR, CGIAR and the European Union; Democratic Republic of Congo), the Lukuru Wildlife Research Foundation (Democratic Republic of Congo), Mbarara University of Science and Technology (MUST, Uganda), WCS-Uganda, the Uganda Forest Department, the Commission of Central African Forests (COMIFAC), the Udzungwa Ecological Monitoring Centre (Tanzania) and the Sokoine University of Agriculture (Tanzania). The AfriTRION network has been supported by the European Research Council (291585, 'T-FORCES' – Tropical Forests in the Changing Earth System, Advanced Grant to O.L.P. and S.L.L.), the Gordon and Betty Moore Foundation, the David and Lucile Packard Foundation and the European Union's Seventh Framework Programme (283080, 'GEOCARBON'). We are grateful to A. Daniels, F. Mbayu, T. R. Feldpausch, E. Kearsley, J. Lloyd, R. Lowe, J. Mukinzi, L. Ojo, A. T. Peterson, J. Talbot and L. Zemagho for giving us access to their plot data. We also thank C. Chatelain (Geneva Botanic Gardens) for access to the African Plants Database and to H. Tang for helping to explore the use of GEDI data. Data from AfriTRON and most of AfriMont are stored and curated by ForestPlots.net, a long-term cyberinfrastructure initiative hosted at the University of Leeds that unites permanent plot records and their contributing scientists from the world's tropical forests. The development of ForestPlots.net and curation of African data have been funded by many sources, including the ERC (principally from AdG 291585 'T-FORCES'), the UK Natural Environment Research Council (including NE/B503384/1, NE/F005806/1, NE/P008755/1, NE/N012542/1 and NE/I028122/1), the Gordon and Betty Moore Foundation ('RAINFOR', 'MonANPeru'), the EU Horizon programme (especially 'GEOCARBON', 'Amazalert') and the Royal Society (University Research Fellowship to S.L.L.).

Author contributions A.C.-S. conceived the study and assembled the AfriMont dataset. A.C.-S. and M.J.P.S. analysed the plot data (with contributions from S.L.L.) and wrote the manuscript. P.J.P. analysed forest extents and contributed to writing. S.L.L. conceived and managed the AfriTRON forest plot recensus programme. E.T.A.M. and V.A. helped compare plot data with remote sensing carbon maps. All co-authors read and approved the manuscript.

Competing interests The authors declare no competing interests.

Additional information

Supplementary information The online version contains supplementary material available at https://doi.org/10.1038/s41586-021-03728-4.

Correspondence and requests for materials should be addressed to A.C.-S.

Peer review information *Nature* thanks Nicolas Barbier and the other, anonymous, reviewer(s) for their contribution to the peer review of this work. Peer reviewer reports are available.

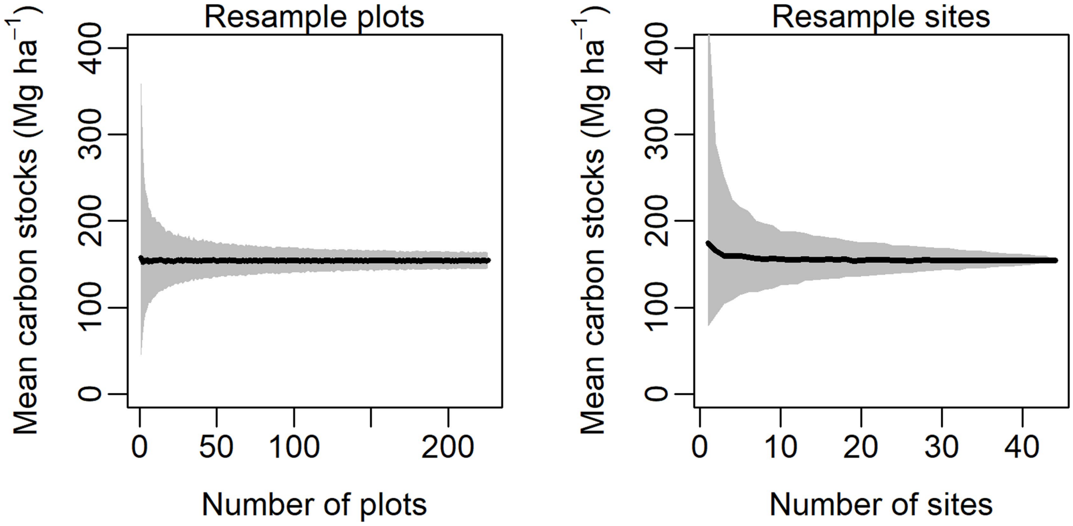

Extended Data Fig. 1 | Sensitivity of mean AGC stock estimates to data subsampling. AfriMont plot data were resampled at different sample sizes either at plot level (sampling with replacement) or at site level (sampling without replacement). $N = 1,000$ resamples for each sample size.

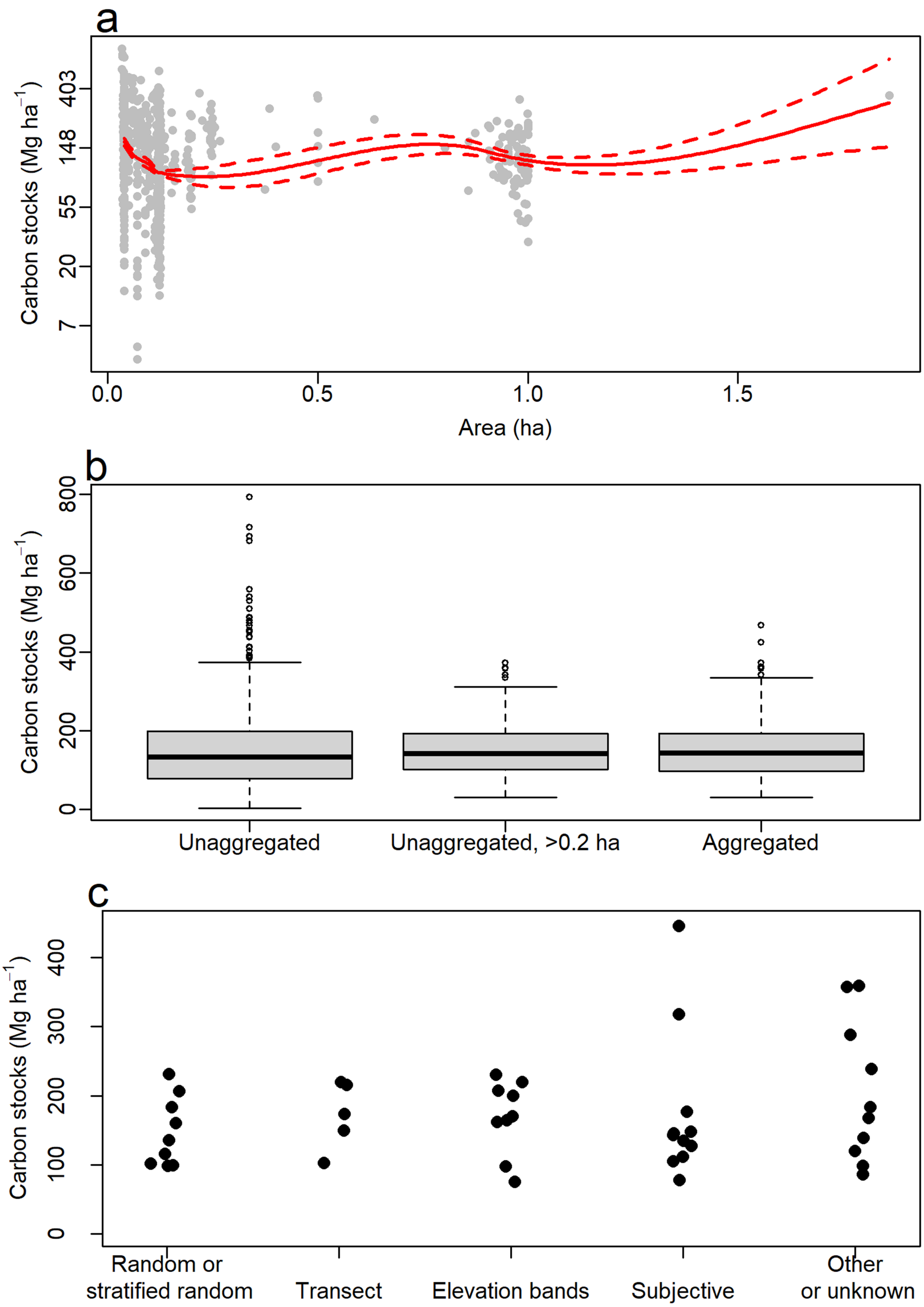

Extended Data Fig. 2 | Effect of plot area, aggregation procedure and plot design on estimates of AGC stocks across the AfriMont plot network. **a**, Relationship between AGC stocks and plot area of plots before aggregation. The red line shows the fit of a locally weighted regression model (span 0.75) relating these variables, with dashed lines showing the standard errors. **b**, Variation in AGC stocks using either all plots before aggregation (unaggregated), plots before aggregation but excluding those <0.2 ha (unaggregated, >0.2 ha) or the aggregated plots used in the main analyses (aggregated). **c**, Effects of plot design on AGC stocks (each site represents one dot). Sampling strategies include random or stratified random, plots positioned along transects, plots established within elevation bands, subjective measures such as choosing an area of forest considered representative of the wider area, and other strategies (one plot sampled per site or unclear strategy). Carbon stocks (log transformed) did not differ significantly between sites with different sampling strategies (analysis of variance $F_{4,39} = 0.432$, $P = 0.785$). For specific site information, see Supplementary Table 5.

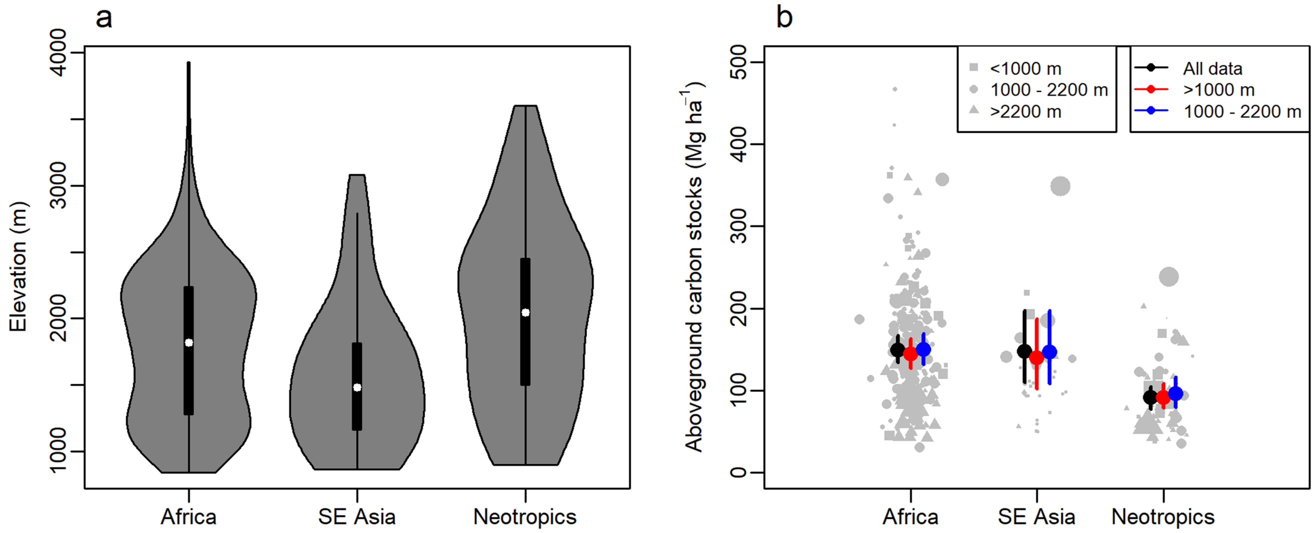

Extended Data Fig. 3 | Robustness of differences in tropical montane forest AGC stocks among continents based on plot networks to differences in elevation. a, Elevations of montane forests plots sampled in each continent. Violin plots show the distribution of data, with boxplots showing the median and interquartile range of elevation in each continent. **b**, Effect of removing submontane plots (800–1,000 m a.s.l.) and high elevation plots (>2,200 m a.s.l., approximately the upper quartile of elevations for the African montane plot dataset) on AGC stocks in montane forests sampled by plot networks in each continent. Mean AGC stocks and 95% CIs are shown as estimated by models using all data, excluding plots 800–1,000 m and restricting plots to 1,000–2,200 m. Means for all plots differ from the analysis in Fig. 1 as literature plots without elevation data (plots in Colombia) were excluded from this analysis. Point symbols are proportional to the square-root plot area. N = 324 plots.

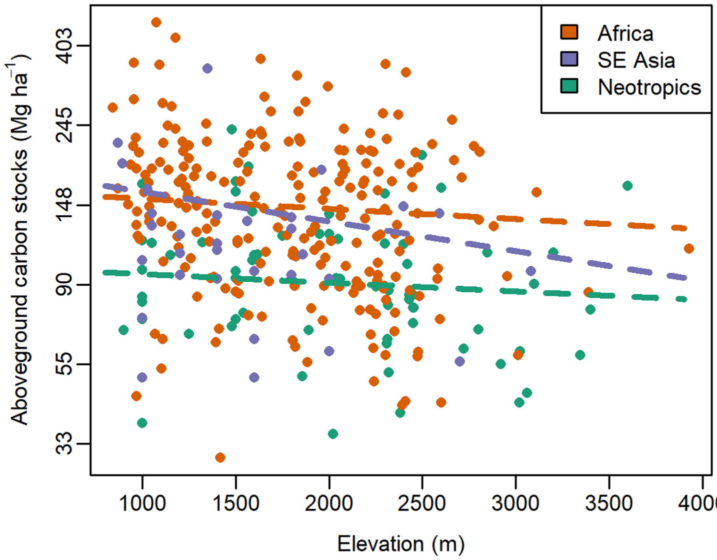

Extended Data Fig. 4 | Relationship between AGC stocks and elevation for tropical montane forests in each continent based on plot networks. The dashed lines show relationships from a linear mixed-effects model of log-transformed AGC stocks as a function of elevation, continent and their interaction. Site was included as a random effect, and AGC stock–elevation relationships allowed to vary among sites. The lines show fitted slopes across sites. Neither the overall relationship between elevation and AGC stocks (slope −0.039 [95% CI = −0.127–0.057], P = 0.420) nor interactions between elevation and continent (Southeast Asia, change in slope = −0.074 [−0.294–0.149], P = 0.503; Neotropics, change in slope 0.006 [−0.132–0.149], P = 0.913) are statistically significant. N = 324 plots.

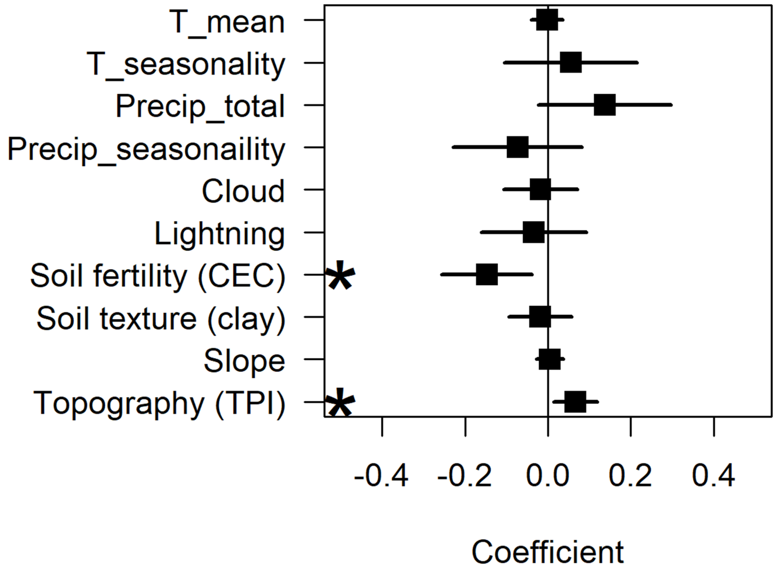

Extended Data Fig. 5 | Environmental drivers of AGC stocks across the AfriMont plot network. Coefficients are from a linear mixed-effects model with site as a random intercept. Results are following all-subsets regression and model averaging, in which variables that do not appear in well supported models are given coefficients of zero, leading to shrinkage in model coefficients. Statistically significant relationships ($P < 0.05$) are indicated with asterisks. TPI refers to topographic position index (positive values indicate higher than surroundings and negative values indicate lower than surroundings). T_mean, annual mean temperature; T_seasonality, temperature seasonality; Precip_total, annual precipitation; Precip_seasonality, precipitation seasonality.

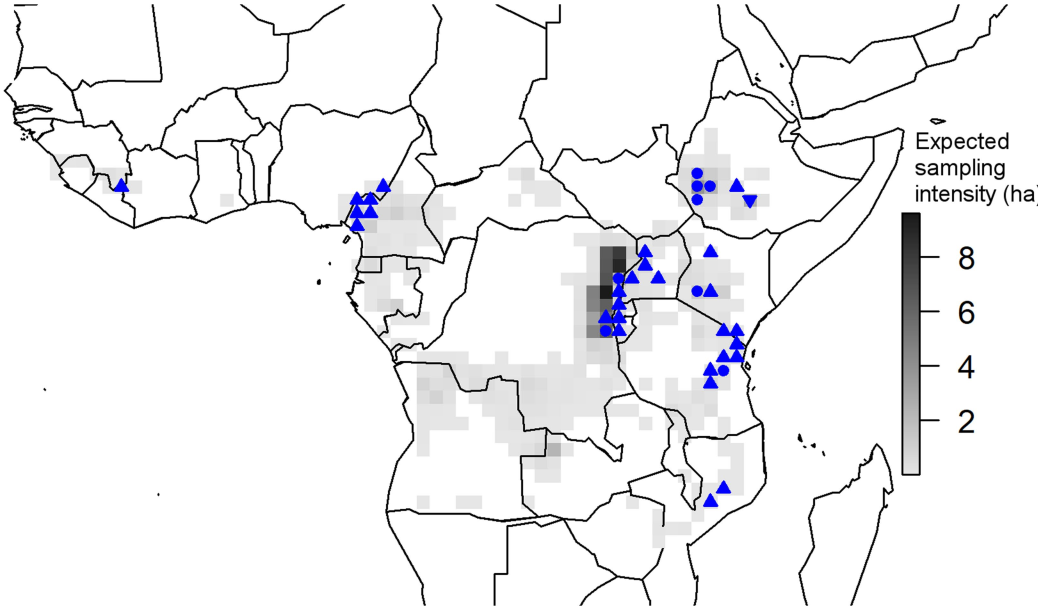

Extended Data Fig. 6 | Expected sampling effort if effort was distributed in proportion to the area of tropical montane forest biome in Africa. Data are summarized at 1° resolution. The upward triangles show grid cells where AfriMont sampling effort is more than double expected effort and the downward triangles show grid cells where AfriMont sampling effort is less than half expected effort. The circles denote AfriMont sampling effort being between half and double expected effort. The extent of the tropical montane forest biome was defined as closed-canopy forests ≥800 m a.s.l. in December 2018, extracted from ref. [38] and clipped to 'primary humid forest' using ref. [39]. This grided map differs from Fig. 4 as numerous grids have very little tropical montane forest.

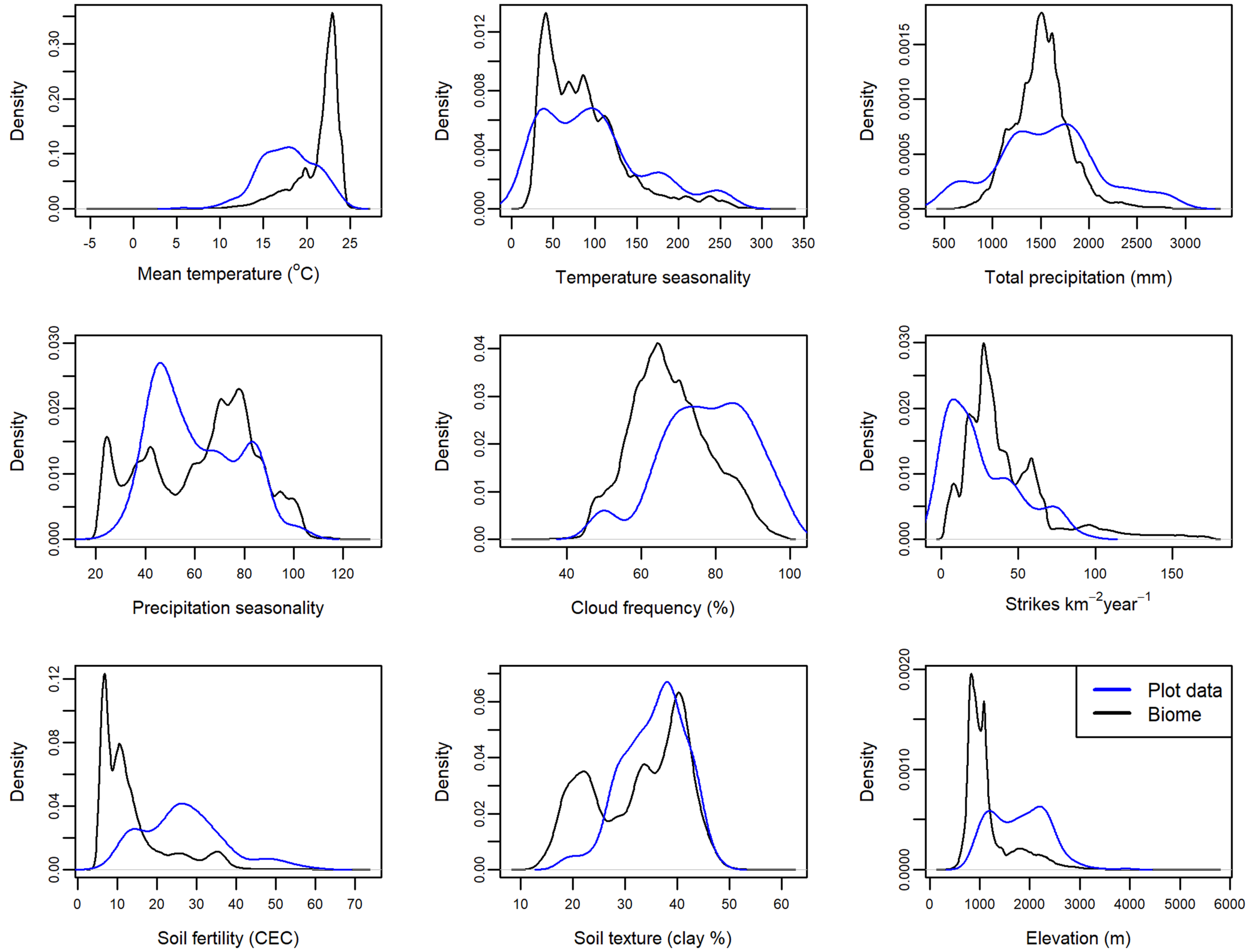

Extended Data Fig. 7 | Differences in the environmental conditions sampled by the AfriMont plot network and the tropical montane forest biome in Africa. The extent of the biome was defined as closed-canopy forests ≥800 m a.s.l. in December 2018, extracted from ref. [38] and clipped to 'primary humid forest' using ref. [39]. Environmental variables for the biome were extracted at about 1-km resolution.

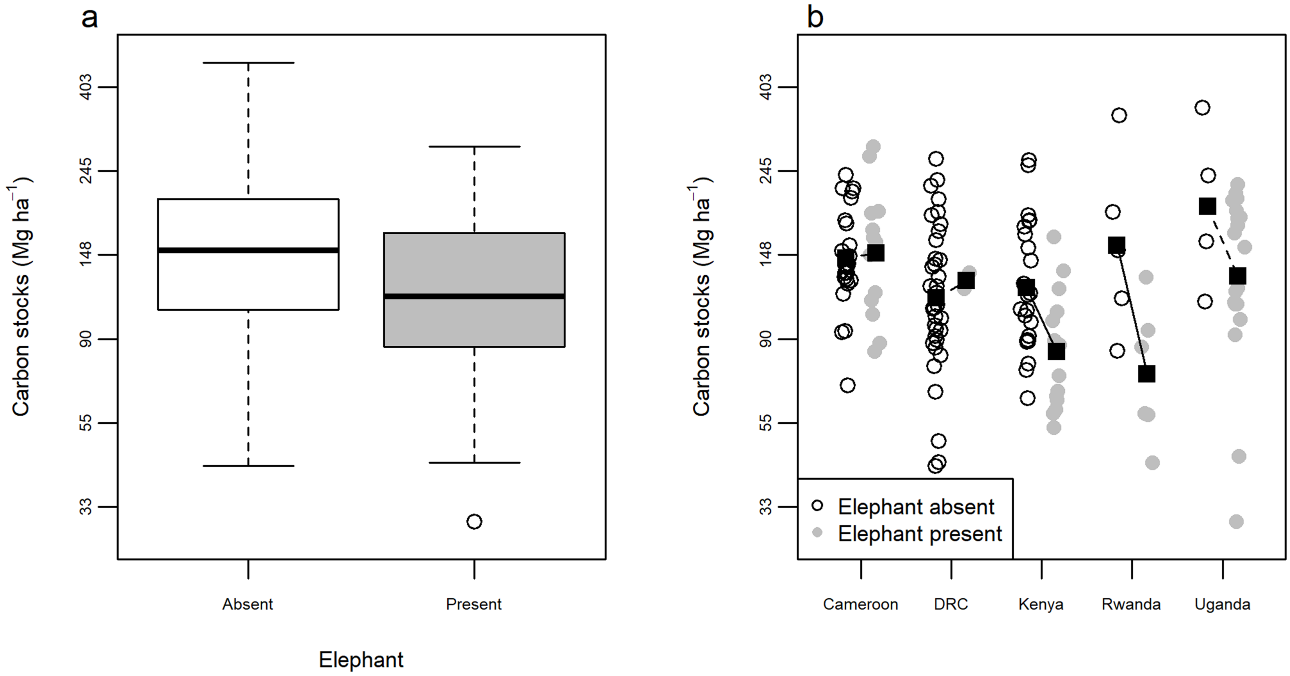

Extended Data Fig. 8 | Differences in AGC stocks in AfriMont plots located in montane forests with and without elephants. a, Differences across all plots. AGC stocks are statistically significantly lower in forests with elephants (*t*-test, $t = 3.5$, d.f. = 83.5, $P = 0.001$). The thick line shows the median, and boxes cover the interquartile range (IQR). Values >1.5 times IQR away from the IQR are shown by points. **b**, Differences in countries where elephants are present in at least one of the montane sites studied. The black squares show means in each country in forests with or without elephants and the solid lines denote statistically significant differences (*t*-tests, $P < 0.05$). Elephant presence in 2019 was estimated by the co-authors (Supplementary Table 5).

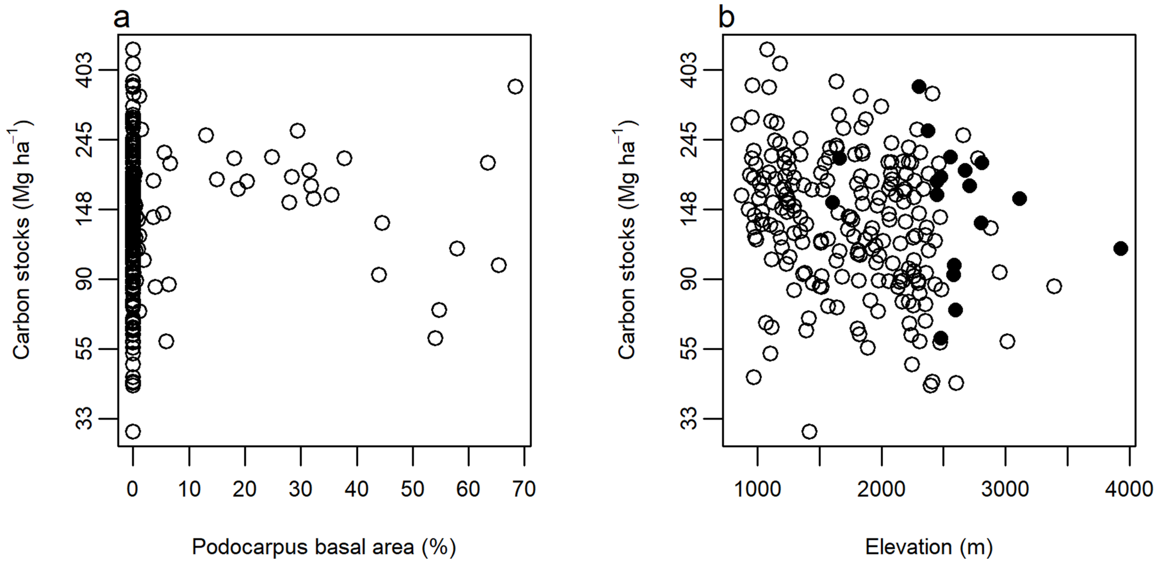

Extended Data Fig. 9 | Relationship between AGC stocks and Podocarpaceae. **a**, Relationship between AGC stocks and Podocarpaceae basal area across plots in the AfriMont network, expressed as a percentage of total plot basal area. These variables are not significantly correlated (r_s = 0.083, n = 226, P = 0.212). **b**, Distribution of plots with at least 20% basal area of Podocarpaceae (black points) in relation to elevation and AGC stocks. AGC stocks are not significantly related to elevation or Podocarpaceae basal area (linear mixed effects model, P = 0.152 and P = 0.132, respectively).

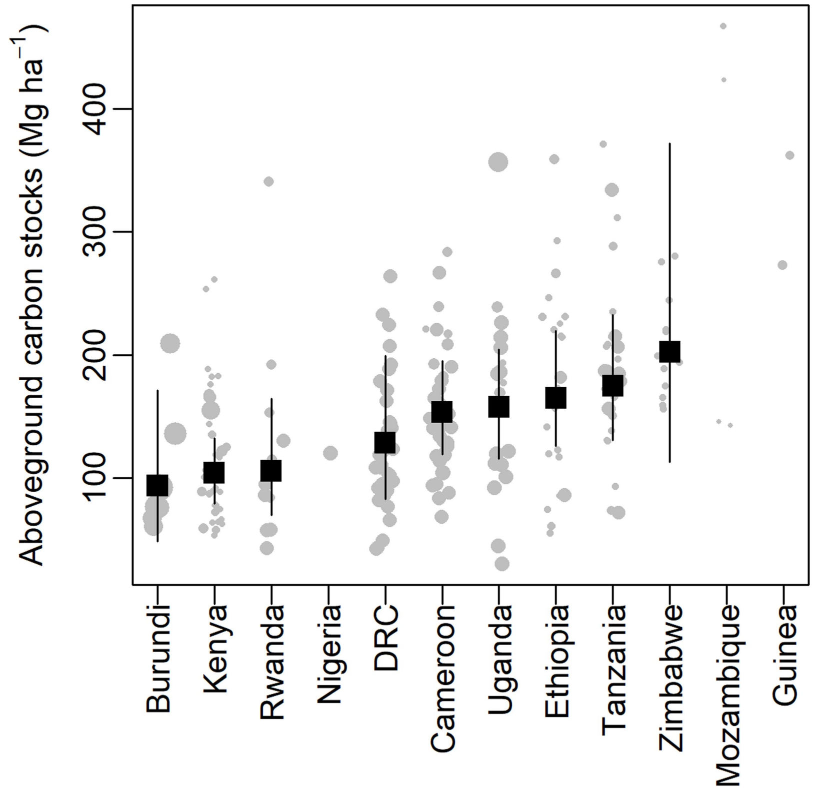

Extended Data Fig. 10 | Within-country variation in AGC stocks based on the AfriMont plot network. Error bars show means and 95% CIs estimated by linear mixed-effects models. Modelled means not shown for countries with fewer than five plots. Point size is proportional to plot area.